



Contents lists available at ScienceDirect

## Nuclear Instruments and Methods in Physics Research B

journal homepage: [www.elsevier.com/locate/nimb](http://www.elsevier.com/locate/nimb)

# Design and characterization of a mapping device optimized to collect XRD patterns from highly inhomogeneous and low density powder samples

A. D'Elia<sup>a,b</sup>, G. Cibin<sup>c</sup>, P.E. Robbins<sup>c</sup>, V. Maggi<sup>d,e</sup>, A. Marcelli<sup>f,g,h,\*</sup><sup>a</sup> Università degli studi Roma Tre, Largo S. Leonardo Murialdo 1, 00146 Roma, Italy<sup>b</sup> University of Trieste, Department of Physics, 34127 Trieste, Italy<sup>c</sup> Diamond Light Source, Harwell Science and Innovation Campus, OX11 0DE Didcot, Oxfordshire, UK<sup>d</sup> Dipartimento di Scienze dell'Ambiente e della Terra, Università degli Studi di Milano Bicocca, Piazza dell'Ateneo Nuovo 1, 20126 Milano, Italy<sup>e</sup> INFN - Sezione di Milano Bicocca, Piazza della Scienza 2, 20126 Milano, Italy<sup>f</sup> INFN Laboratori Nazionali di Frascati, P.O. Box 13, 00044 Frascati, Italy<sup>g</sup> RICMASS, Rome International Centre for Materials Science Superstripes, 00185 Rome, Italy<sup>h</sup> CNR-ISM, LD2 Unit, Via del Fosso del Cavaliere 100, 00133 Rome, Italy

## ARTICLE INFO

## Article history:

Received 12 November 2016

Received in revised form 16 February 2017

Accepted 11 March 2017

Available online 25 April 2017

## Keywords:

X-ray diffraction

Mapping

Antarctica

Rotating positioner

Dust

## ABSTRACT

We report on the development of a device designed to improve X-ray Powder Diffraction data acquisition through mapping coupled to a rotational motion of the sample. The device and procedures developed aim at overcoming the experimental issues that accompany the analysis of inhomogeneous samples, such as powders, dust or aerosols deposited on a flat substrate. Introducing the mapping of the substrate on which powders are deposited and at the same time the rotation, we may overcome drawbacks associated to inhomogeneous distributions such as ring-like patterns due to the coffee stain effect generated by the evaporation of a solution. Experimental data have been collected from powders of a NIST standard soil sample (11 µg) and from an airborne dust extracted from deep ice cores in Antarctica (9.6 µg). Both particulate samples have been deposited on polycarbonate membranes from ultra-dilute solutions. Data show that this approach makes possible to collect XRD patterns useful to identify mineral fractions present in these low density samples.

© 2017 Elsevier B.V. All rights reserved.

## 1. Introduction

Obtaining information about the mineralogical composition of natural samples characterised by very small amounts of material poses significant analytical challenges. A microscopic approach, as possible with modern electron microscope techniques such as high-resolution Transmission Electron Microscopy (HR-TEM) is often successful, as allows identifying individual particles' composition and structure [1]. However, this relies on the ability to extract and deposit microscopic particles on small supports (e.g., e.m. grids), on the identification of individual particles and on the collection of large datasets to guarantee a significant statistical sampling.

\* Corresponding author at: INFN Laboratori Nazionali di Frascati, P.O. Box 13, 00044 Frascati, Italy.

E-mail address: [marcelli@lnf.infn.it](mailto:marcelli@lnf.infn.it) (A. Marcelli).

At the same time, the extraction procedures for preparation to microscope analysis add manipulation steps exposing samples to potential contaminations. In addition, the need to expose micron-sized materials to vacuum conditions for relatively long acquisition sessions cannot guarantee minerals are found in their pristine state, which is particularly true in hydrated systems or in general for samples where equilibrium with the environment is important. On the other side, application of averaging analytical methods, where X-ray Powder Diffraction (XPRD) plays a major role, potentially faster and more statistically significant, is restricted by the detection limit boundary. High samples' dilution, i.e., the dispersion of minute amounts of significant material over large deposition areas, lowers the signal/background figure as samples' support contribution to the measurement becomes dominant.

In this work as example, polycarbonate filters affected data by an intense background signal, which decreases drastically the signal/noise ratio. One way to help overcoming this problem, is to use intense and collimated sources as provided by synchrotron

radiation instead of laboratory sources. The high photon flux ( $\sim 10^{11}$  monochromatic photon/s still using a synchrotron radiation bending magnet source from a modern facility) and the high brilliance giving well collimated and small beams increases significantly the possibility to detect weak peaks while decreasing significantly the acquisition time. As a comparison, reference information on low concentration dust samples of nature similar to the examples presented here (with concentrations comparatively higher by a factor 6 to 50), but using conventional instrumentation and consequently long acquisition times (hours) can be found in references [2–4].

This is particularly significant in the case of the analysis of the insoluble mineral fraction extracted from deep ice cores. In cold areas far from direct anthropic and natural contamination, the mineral particulate trapped in snow efficiently samples the dust circulating in the atmosphere. Dust extracted from ice cores, taken

from locations where snow and ice accumulation is regular and unperturbed, represents then a time-lapsed profile of the atmospheric composition. Deep ice cores from Antarctica [5] span among the longest temporal window, and provide information on the earth climate with high temporal resolution, back to one million years before present.

Analysis of this particulate poses substantial analytical challenges. Concentration of the mineral fraction is particularly low, as figures of 10–100 ng of mineral particles per g of ice are the norm. Therefore, extraction and concentration of this extremely low quantity of solid particles make sample preparation difficult and prone to external contamination. To minimise contamination in particular, a single preparation step providing samples good enough for different analytical techniques is the ideal route. In our case, samples are prepared with the minimal number of sample manipulation steps, by direct filtration of melted ice on polycarbonate membranes of diameter 13 mm. The polycarbonate substrate was chosen in order to perform both mineralogical and elemental composition analyses of mineral materials coupling XPRD, Proton Induced X-ray Emission (PIXE) [6], and subsequently synchrotron-based X-ray Fluorescence (XRF) and X-ray Absorption Spectroscopy (XAS) analyses [7]. Elemental purity was a driving parameter for the choice of the material for PIXE and XRF analyses, giving essential elemental information for the characterisation of aerosol materials.

For XPRD analysis the use of polycarbonate filters causes the presence of a non-negligible background, with a strong scattering peak evident at 20 degrees for acquisitions with incident beam energy at 7 keV. A previous approach [2,3] using a standard X-ray tube and a PANalytical X'Pert Pro diffractometer equipped with a multi-channel X'Celerator detector in parallel beam geometry, has demonstrated that it is nonetheless possible to recognise main mineral fractions in Antarctic samples with accurate preparation and long acquisition times (several hours), with a detection limit estimated to be  $\sim 1 \mu\text{g}$  per mineral fraction. Using this approach, the average peaks' number observed in the whole pattern ranges from 3 to 5 for dust depositions of the order of  $100 \mu\text{g}$ . Improving over this limit is possible only by considering the sources of signal limitation in the data acquisition strategy. In the case of low concentrated systems, the signal/noise ratio is dominated by the diffuse scattering of the sample support always present while the

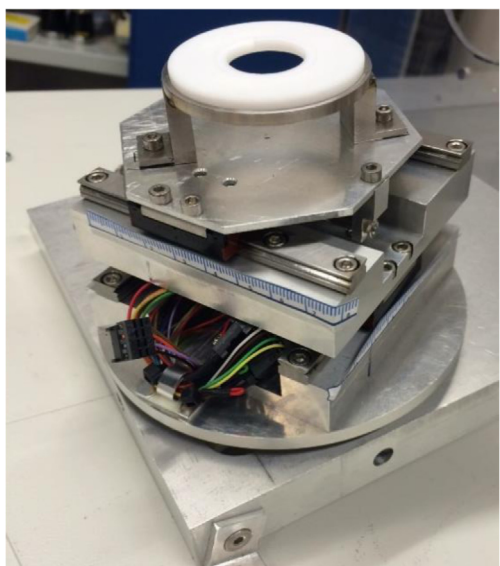


Fig. 1. Photograph of the assembled Antarctica Sample Project X-ray positioner (ASPjX).

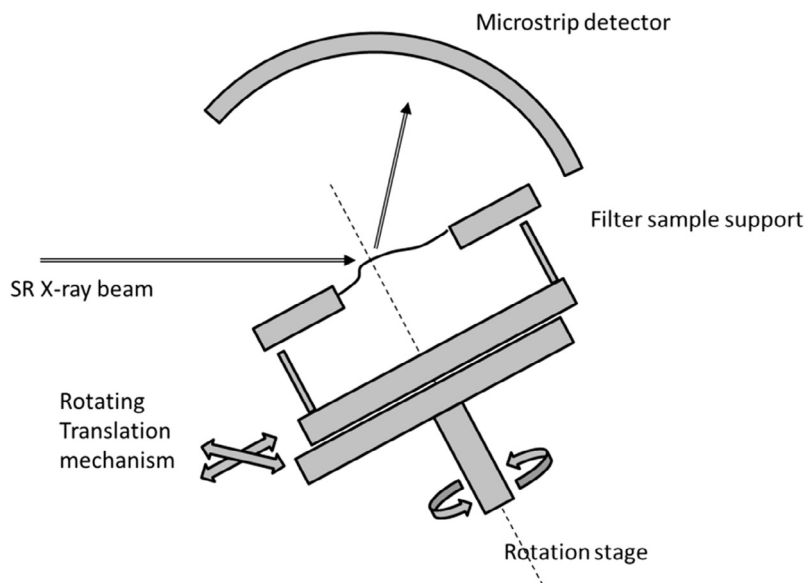


Fig. 2. Schematic description of scanning mechanism and detection geometry of the sample manipulation device.

signal is potentially consisting of a sum of sparse intense reflections from individual diffracting crystallites. Those, when averaged over the sampled area (the polycarbonate filter) result in a weak XPRD pattern with low statistical significance when compared to the background integrated intensity. In fact, using a different substrate (e.g., metal surfaces) for dust deposition the signal/noise ratio increase remarkably [4]. Since, as underlined before these samples have been also investigated through XRD, PIXE and XAS it has not been possible to use a metal surface or a more convenient material than polycarbonate. Therefore, we decided to adopt an acquisition protocol similar to the microscopic approach, i.e., using a focused beam to illuminate a small fraction of the surface area, in principle allows getting a higher contrast between the signal and the background. To obtain statistically significant XPRD datasets is important to consider sample deposition inhomogeneity. As mineral dust is deposited through filtration and water evaporation on polycarbonate filters from a dilute solution ( $\sim 100 \mu\text{g/l}$ ), the solution evaporation dynamics often gives rise to the formation of so-called coffee stain patterns [8], which can separate mineral

fractions in different areas of the filter. Mapping the full surface area is therefore essential. Our approach has been to develop a device that allows acquiring a full map of the filter, while at the same time preserving the possibility to spin the sample and maintaining the incoming beam over a fixed centre of rotation.

## 2. Experimental

As mentioned, conventional XPRD experimental set ups [9] for flat plate geometry usually provide a slow rotation ( $\sim 1^\circ/\text{s}$ ) of the sample [2,3]. Typically, a parallel unfocused beam, illuminates uniformly the flat plate sample to guarantee a large coverage, while spinning helps sampling a large crystal orientation area in the reciprocal lattice space, maintaining the flat plate geometry. Using these experimental configurations, the number of diffraction peaks detected in previous works on Antarctic ultra-dilute samples, consisting of about 10–100  $\mu\text{g}$  of deposited dust, has been found to be in the range from 3 to 5 in a whole XRD pattern [2,3]. It must be noted that this is a limitation especially for clay minerals, where

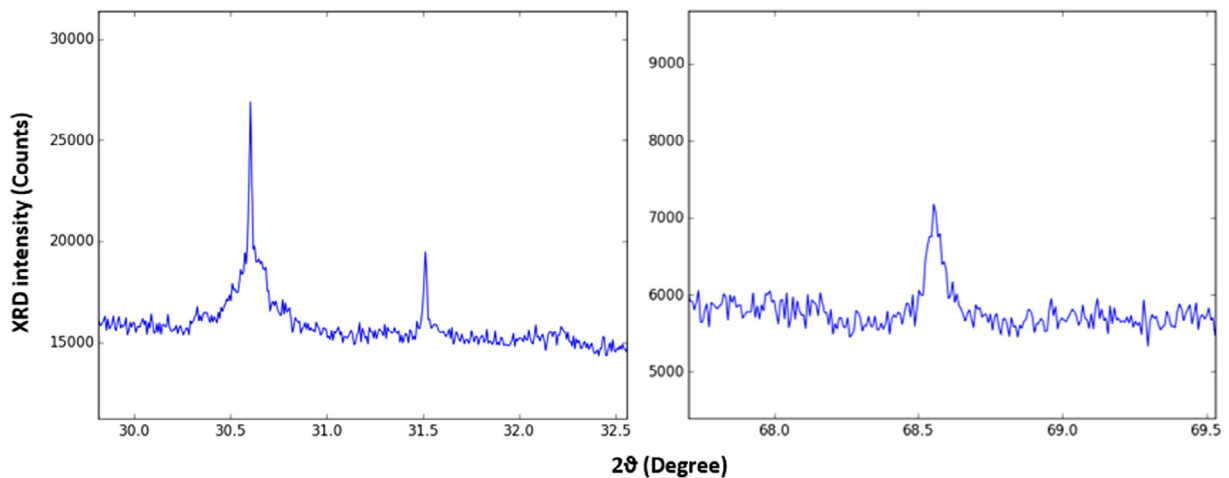


Fig. 3. Peaks detected in the angular regions of 30–32.5° (left panel) and 67.5–69.5° (right panel) for a single point XRD acquisition of the NIST2709a (11  $\mu\text{g}$ ) standard.

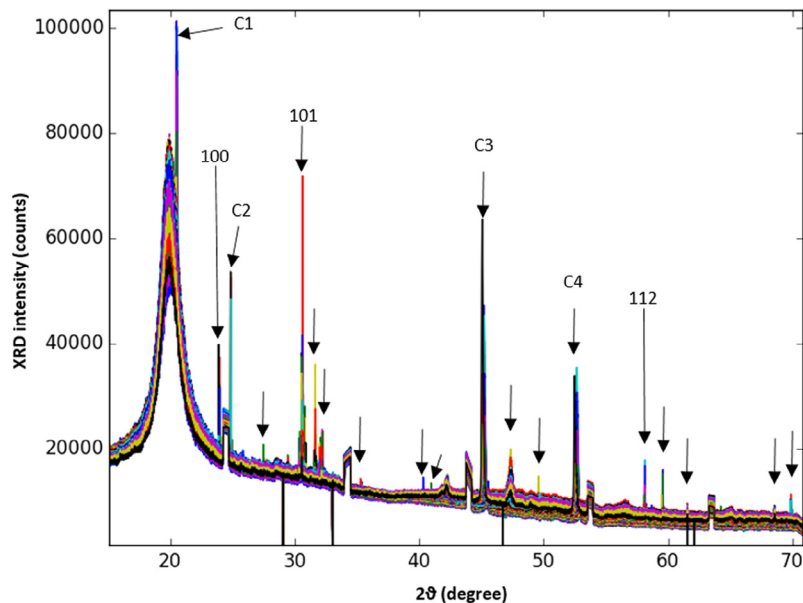


Fig. 4. XRD patterns collected on the NIST2709a standard using a grid of 84 points. Three reflections due to the  $\alpha$  phase of quartz can be identified and labelled with their Miller indices. Four peaks (C1–C4) are not identified while the broad peak at  $20^\circ$  is due to the contribution of the amorphous polycarbonate filter.

a minimum number of three reflections is suggested for a full identification [10]. This difficulty is expected, as the sample composition and structure pose additional difficulties for the XRD measurements as well.

The aerosol deposited in deep ice cores shows low crystallinity, as is mainly composed of soft clay minerals (which are preferentially transported over long distances) and it is expected that post-deposition alteration mechanisms can affect the long range structure of the mineral fractions. Most of the XRD signal detectable above the support continuum background is therefore expected to come from reflections by individual particles of relatively large size and therefore high crystallinity. An acquisition strategy based on the repeated acquisition of XRD frames, mapping the sample deposition area with a small beam focus can therefore maximise the probability of identifying such reflections, benefitting of a better signal/background ratio.

To verify this approach, we realised a sample manipulation device that allows a raster scan of the sample while undergoing a full continuous rotation. The sample holder is placed on top of an (X,Y) scanning mechanism, which is assembled on a circular rotating base (Fig. 1). In this configuration, the entire scanning system and the sample holder are rotated around a vertical axis. A sample translation therefore does not alter the position of the rotation axis. Alignment of the X-ray beam to the centre of rotation of the surface area, allows illuminating continuously only the portion of sample that is located on the rotation axis. This configuration therefore allows to illuminate different portions of the sample, keeping rotation and a minimal beam footprint on each sample position. It is then possible to collect data from the whole area where the sample is deposited, overcoming the issue of the inhomogeneous deposition.

We used as a reference sample for dilute sample acquisitions NIST2709a, a standard soil of the San Joaquin valley (U.S.A.) from the National Institute of Standards and Technology (NIST) [11,12]. To mimic the sample preparation used for the extraction of ice core dust the soil was first dispersed in distilled water (18.2 M $\Omega$ ) to obtain a density <100  $\mu\text{g/l}$ . The suspension was deposited drop by drop using a pipette on a *Nuclepore* polycarbonate membranes with a pore size of 0.45  $\mu\text{m}$  and a diameter of 13 mm, following the procedure used for the deposition of Antarctic samples aimed at getting a high dust concentration minimising the deposition area. Extraction of water was accelerated with the aid of a vacuum pump, and the filter was left to dry in air.

This deposition method does not avoid anyway the dust accumulation in concentric rings [8] as it is observed in a wide range of solutions and solute concentrations. In order to minimize the incidence of the coffee stain effect, future samples' deposition will be performed via microdrop deposition technique [13] to obtain a concentrated dust distribution in a small area of the filter. The rotating system is powered by a 12 V DC motor connected to the rotating circular base. For the experiments, the base was moving at a fixed velocity of 60 rpm. The scanning system is composed of two translation stages, with a travel range of 48 mm, long enough to ideally scan the entire surface area of the sample. The stages, supported by four 89 mm rails, and compact recirculating ball bearing carriages, are driven by two bipolar 20DAM-K Portescap 8.9 N 12 V stepper linear actuators, with a drive length of 48 mm. The rails and stepper assembly are mounted in a cross configuration designed to minimise the overall manipulator height (see Fig. 2).

Control to the (X,Y) mapping stage was provided through the rotation axis using a slip ring, with 12 rotating electrical contacts. Eight poles are used for the scanning system motors power supply and four for travel limit switches.

XRD patterns were acquired on B18, the Core XAS beamline at Diamond Light Source, the UK national synchrotron radiation facility. For this experiment, the double crystal monochromator

equipped with Si111 crystals was used to provide monochromatic beam with resolution  $\Delta E/E \sim 1.4 \times 10^{-4}$  [14]. On B18, a toroidal mirror provides focused X-ray beam with size adjustable from  $1 \times 1 \text{ mm}^2$  down to approximately  $100 \times 100 \mu\text{m}^2$ , and divergence at the sample position of  $0.4 \times 2.2 \text{ mrad}$  in the vertical and horizontal directions, respectively. XRD patterns were acquired using a Dectris Mythen Si microstrip detector system. The detector is composed of an array of six modules, for a total of 7680 microstrip

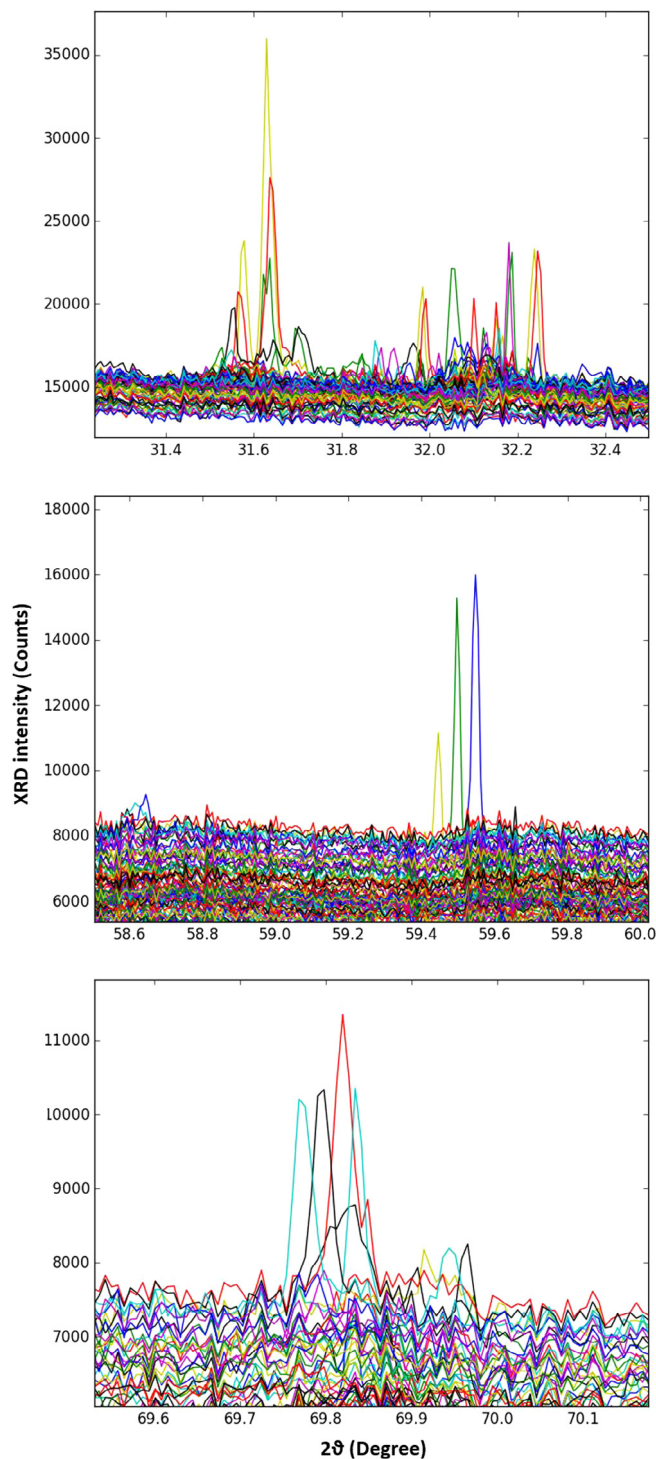


Fig. 5. Comparison among patterns of the NIST 2709a standard (11  $\mu\text{g}$ ). From top to bottom the angular ranges: A) 31.4°–32.4°, B) 58.6°–60° and C) 69.6°–70.1°.

sensors, arranged in an arc covering  $60^\circ$  to provide in the  $2\theta$  geometry an average angular resolution of  $0.008^\circ$ .

### 3. Results

To evaluate the device and the support contribution to the XRD data acquisition on ultra-low concentrated and inhomogeneously deposited samples, we have first investigated a sample composed of  $11 \mu\text{g}$  of dust of the standard soil NIST2709a. We collected the XRD patterns putting the sample on rotation ( $\sim 360^\circ/\text{s}$ ) at the beam energy of 7 keV with an acquisition time of 60 s. The beam was partially defocused in this case, with dimensions of  $0.6 \text{ mm} \times 0.5 \text{ mm}$  (HxV). Angular regions where significant powder diffraction signals can be detected from a single point acquisition are shown in Fig. 3.

A limited number of peaks can be barely detected over a strong background signal, due to the contribution of the polycarbonate filter on which dust is deposited. As a comparison, we explored a rectangular grid of 84 points with focused beam on the same sample, using the same acquisition parameters.

Fig. 4 clearly points out the increase of the number and of intensity of the peaks respect to the three features detected in the original pattern. From the analysis of these patterns at least 19 reflections can be detected, with an increase of more than six times respect to the case without translation. The background signal varies along different positions of the grid. This is due to the fact that different sample concentration areas are illuminated, contributing to the overall scattering background with different intensities. Peaks C1–C4 indicated in Fig. 4 are not present in the standard XRD pattern of the NIST2709a [11]. These additional peaks are most likely due to contamination from the sample manipulation.

As visible in Fig. 4, three peaks at  $24.0^\circ$ ,  $30.7^\circ$  and  $58.3^\circ$  can be clearly identified and we associated them to the quartz  $\alpha$  phase. Assuming quartz abundance in the soil deposited on the filter to reflect the average fraction of  $\sim 12\%$  of the mass of the Earth's crust, this would indicate that in our experimental conditions (84 acquisitions, 60 s each) an upper value for the detection limit of quartz could be set between 1 and  $2 \mu\text{g}$ .

Fig. 5 shows how measured peaks most likely to be assigned to similar mineral fractions exhibit different angular positions when acquired on different points of the grid. This is most due to an

imperfect flatness of the sample holder. A variation in height of the sample on the rotation axis causes indeed a horizontal displacement of the beam position along the propagation direction and an enlargement of the beam footprint. These contributions affect the XRD pattern with an uncertainty in the peak position of  $\sim 0.1^\circ$ . It has to be noted that this is a limit set by the configuration of the present prototype, where no adjustments of the sample vertical position have been implemented (Fig. 2). Development of a diagnostics system and sample height correction mechanism will minimize this systematic angular error.

As reference for comparison of the standards' data to realistic aerosol samples, we present finally a series of XRD patterns measured on a sample consisting of  $9.6 \mu\text{g}$  of dust from a deep ice core from Antarctica, deposited using the same protocol on a *Nuclepore* polycarbonate filter (see Fig. 6).

Mineral composition studies have been conducted in the past years and are still in progress to understand the provenience of dust through the different climatic periods [15,16]. As underlined in the introduction, XRD on these samples is particularly challenging. For the present measurement, data acquisition has been performed on a square grid of 81 points with steps of 0.5 mm in both directions covering an  $8 \times 8 \text{ mm}$  area. For each point of this grid, an XRD pattern has been collected again at 7 keV with an acquisition time of 60 s. The beam dimension was  $0.6 \text{ mm} \times 0.5 \text{ mm}$  (HxV) and the angle of the sample respect the X-ray beam was set to  $15^\circ$ . The XRD pattern shows that 9 reflections can be resolved (position of the detected XRD peaks is indicated by arrows in Fig. 6). The weaker peaks are magnified in the three panels in Fig. 7, and are detected only in some locations, indicating still an irregular deposition and composition of the dust collected on the filter.

Because of their characteristics, clays are supposed to be the most common mineral present in Aeolian dust [17]. In order to observe the possible presence of clay minerals, we modified the detector angle respect to the X-ray beam direction from  $15^\circ$  to  $2^\circ$  trying to detect diffraction contributions at lower angles. Indeed, since clays are characterized by a 3D molecular arrangement with a high d-spacing ( $\sim 10 \text{ \AA}$ ) their main peaks are usually detected at low angles [18]. The different experimental conditions increased the background and slightly modified the shape of the pattern respect to the previous test. Within the detection limit, the result points out the lack of clay minerals and the need to improve the experimental set up to better investigate the lower angles region.

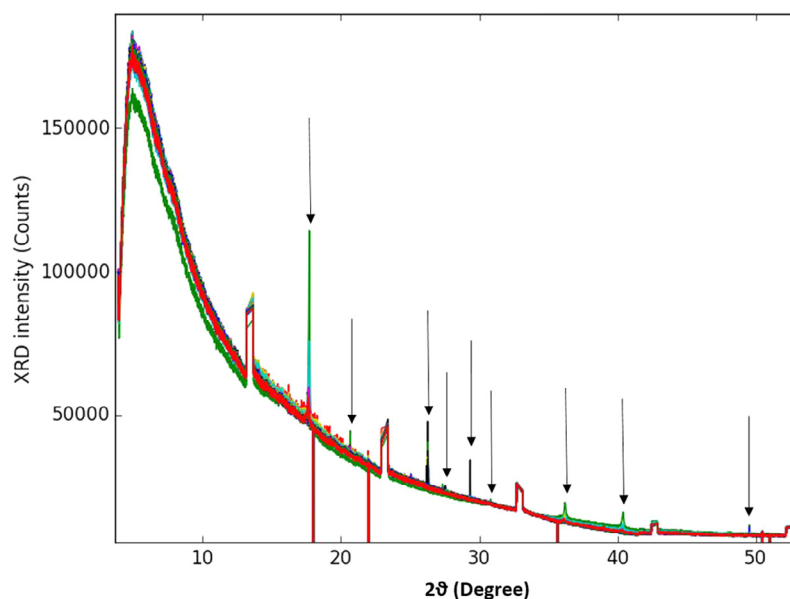
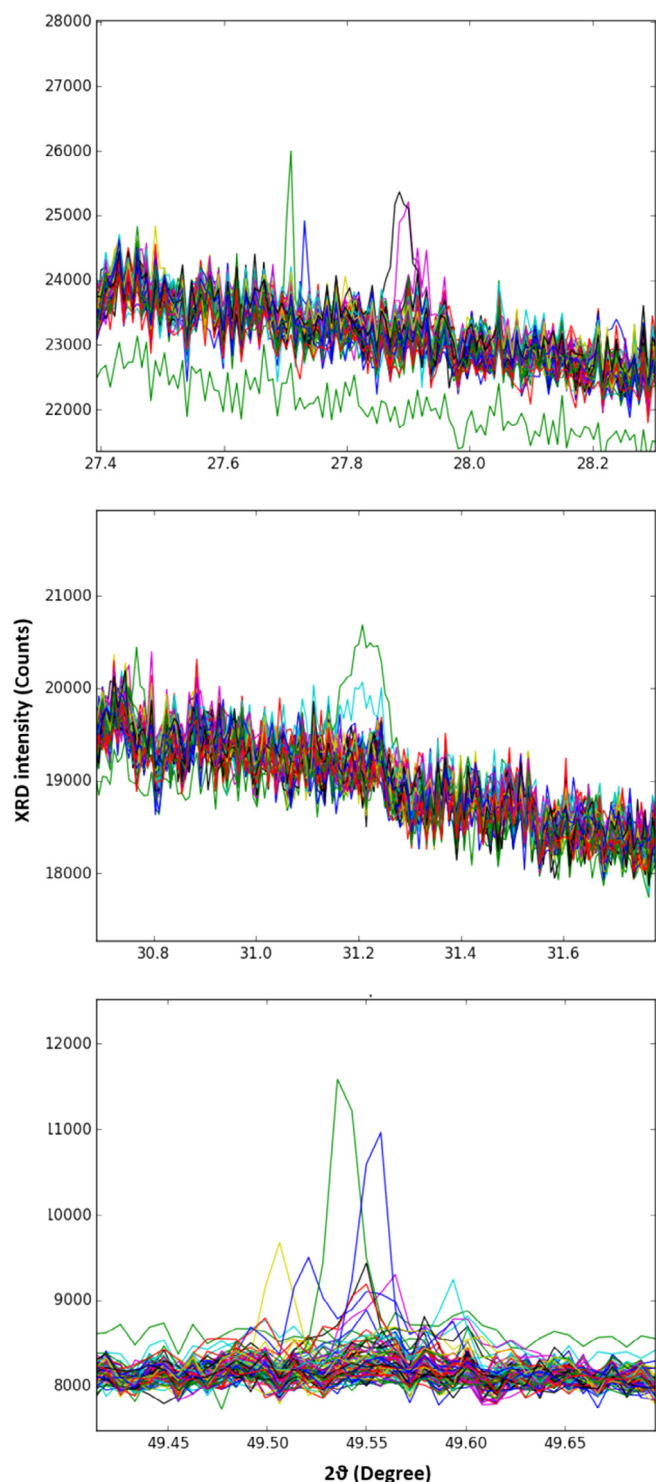


Fig. 6. XRD patterns collected on the sample containing Antarctica dust (Sample 14) using a square grid of 81 points.



**Fig. 7.** The weak peaks of the sample containing Antarctica dust in different angular ranges; A) 27.4–28.2°, B) 30.8–31.6°, C) 49.95–50.3°. Some of these peaks are present only in specific locations of the grid.

#### 4. Conclusions

Data presented and discussed in this contribution illustrate the potential advantages of a mini-focus beam setup that, when coupled to a translation system allowing for an on-axis sample rotation, allows increasing the number of diffraction peaks detectable above the continuous background produced by a light and amorphous support, from a sample composed of fine particles dis-

persed on a relative large area. For the standard soil NIST2709a, this number increases from 3 to 15 with a deposition of 11  $\mu\text{g}$  while it goes from 0 to 9 for a sample containing 9.6  $\mu\text{g}$  of Antarctica dust.

Comparing these results with those obtained using a conventional laboratory diffractometer along with a laboratory X-ray source and investigating samples up to 10 times denser with a longer acquisition time (several hours) this new approach demonstrated that a higher detection efficiency can be obtained. The increased number of peaks quantity and the increased signal/noise ratio obtained with the new device, makes possible the identification of the mineral fraction present in this kind of sample and thus opens new analysis' possibility such as structure refinement via Rietveld method. From a rough estimation (due to the limited statistics on the number of diffraction peaks detectable) we set a preliminary value for the lower limit of mass detection to an average value greater than 1.5  $\mu\text{g}$  for 60 s/point acquisitions using a modern bending magnet source. Although work is still in progress to improve the performance of this device, the results achieved are encouraging. The vertical adjustment of the sample is essential to enable an accurate angular calibration and to avoid the widening of the footprint of the beam due to irregularities of the surface of the membrane. This effect cannot be ruled out, as the displacement from the diffractometer centre of  $\sim 1$  mm introduces a non-linear angular offset of the diffraction pattern of  $\sim 3^\circ$ . These drawbacks are important for the analysis, but do not represent a physical limitation. They can be certainly fixed or minimized when considering also the recent developments in the procedures for concentrated deposition of these particularly challenging and delicate samples.

#### Acknowledgments

We strongly acknowledge B. Del Monte and G. Baccolo for their invaluable support in the preparation of the ultra-dilute sample from Antarctica. One of us (A.D.) sincerely thanks the Diamond Light Source for accepting his thesis scholarship and for partial financial support.

#### References

- [1] A. Laskin, J.P. Cowin, M.J. Iedema, Analysis of individual environmental particles using modern methods of electron microscopy and X-ray microanalysis, *J. Electron Spectrosc. Relat. Phenom.* 150 (2006) 260–274.
- [2] Marco Sala, PhD thesis, Mineralogy of Antarctic ice dust and Potential Dust Source Areas in the Southern Hemisphere, Department of Earth Sciences Arditio Desio, Milan University, 2007–2008.
- [3] M. Dapiaggi, M. Sala, G. Artioli, M.J. Fransen, Evaluation of phase detection limit on filter-deposited dust particle from Antarctic ice cores, *Z. Kristallogr.* 26 (2007) 73–78.
- [4] Ignasi Queralt, Teofilo Sanfeliu, Eva Gomez, Carlos Alvarez, X-ray diffraction analysis of atmospheric dust using low-background supports, *J. Aerosol Sci.* (2001) 453–459.
- [5] F. Lambert et al., Dust-climate couplings over the past 800,000 years from the EPICA Dome C ice core, *Nature* 452 (2008) 616–619.
- [6] F. Marino et al., Defining the geochemical composition of the EPICA Dome C ice core dust during the last glacial-interglacial cycle, *Geochim. Geophys. Geosyst.* 9 (10) (2008) Q10018.
- [7] A. Marcelli, G. Cibin, D. Hampai, F. Giannone, M. Sala, S. Pignotti, V. Maggi, F. Marino, XANES characterization of deep ice core insoluble dust in the ppb range, *J. Anal. At. Spectr.* 27 (2012) 33–37.
- [8] Robert D. Deegan, Olgica. Bakajin, Todd F. Dupont, Greg. Huber, Sidney R. Nagel, Thomas A. Witten, Contact line deposits in an evaporating drop, *Phys. Rev. E* 62 (2000) 756–765.
- [9] B. Tani, S. Siegel, S.A. Johnson, R. Kumar, X-ray diffraction investigation of atmospheric aerosol in the 0.3–1  $\mu\text{m}$  aerodynamic size range, *Atmos. Environ.* 17 (1983) 2277–2283.
- [10] D.M. Moore, R.C. Reynolds, X-ray diffraction and the Identification and Analysis of Clay Mineral, 2nd Ed., Oxford University Press, 1997.
- [11] E.A. Mackey, S.J. Christopher, R.M. Lindstrom, S.E. Long, A.F. Marlow, K.E. Murphy, R.L. Paul, R.S. Popelka-Filcoff, S.A. Rabb, J.R. Sieber, R.O. Spatz, B.E. Tomlin, L.J. Wood, J. H. Yen, L.L. Yu, R. Zeisler, S.A. Wilson, M.G. Adams, Z.A. Brown, P.L. Lamothe, J.E. Taggart, C. Jones, J. Nebelsick, Certification of Three NIST Renewal Soil Standard Reference Materials for Element Content: SRM 2709a San Joaquin Soil, SRM 2710a Montana Soil I, and SRM 2711a Montana Soil II, NIST Special Publication 260–172 (2010) 39 pages.

- [12] Uptakes of Cs and Sr of San Joaquin soil measured following ASTM method C1733, Chemical sciences and Engineering division, ANL-12/11, 2012.
- [13] S. Macis, A. Marcelli, G. Cibin, Microdrop deposition for ultra-diluted samples preparation, in: A. Marcelli, C. Balasubramanian (Eds.), *Nanoscale excitations in emergent materials - NEEM 2015*, Superstripes Press, Rome, 2015, pp. 59–60.
- [14] A.J. Dent, G. Cibin, S. Ramos, A.D. Smith, S.M. Scott, L. Varandas, M.R. Pearson, N.A. Krumpa, C.P. Jones, P.E. Robbins, B18: A core XAS spectroscopy beamline for Diamond, *J. Phys: Conf. Ser.* 190 (2009).
- [15] M. Sala, B. Delmonte, M. Frezzotti, M. Proposito, C. Scarchilli, V. Maggi, G. Artioli, M. Dapiaggi, F. Marino, P.C. Ricci, G. De Giudici, Evidence of calcium carbonates in coastal (Talos Dome and Ross Sea area) East Antarctica snow and firn: *Environmental and climatic implications*, *Earth Plan. Sci. Lett.* 271 (2008) 43–52.
- [16] A. Marcelli, D. Hampai, G. Cibin, V. Maggi, Local vs. global climate change - investigation of dust from deep ice cores, *Spectrosc. Eur.* 24 (2012) 12–17.
- [17] I. Tegen, I. Fung, Modeling of mineral dust in the atmosphere: sources, transport and optical thickness, *J. Geophys. Res.* 99 (1994) 22897–22914.
- [18] *Crystal structures of clay minerals and their X-ray identification*, G.W. Brindley, G. Brown, (Eds.), Mineralogical Society of Great Britain and Ireland, 1980.